Optics Communications 304 (2013) 87–95

Contents lists available at SciVerse ScienceDirect

Optics Communications

journal homepage: www.elsevier.com/locate/optcom

Strong field double ionization by elliptically polarized few-cycle laser pulses

Benhai Yu *, Yingbin Li

College of Physics and Electronic Engineering, Xinyang Normal University, Xinyang 464000, People's Republic of China

ARTICLE INFO

Article history:
Received 12 September 2012
Received in revised form
29 March 2013
Accepted 19 April 2013
Available online 9 May 2013

Keywords:
Double ionization
Elliptically polarized few-cycle laser pulse
Carrier-envelop phase
Ionization time

ABSTRACT

With the classical ensemble model, we have investigated double ionization of xenon atoms by an elliptically polarized few-cycle laser pulse at intensity 4×10^{14} W/cm^2. The results show that sequential double ionization (SDI) and nonsequential double ionization (NSDI) exist simultaneously with this laser field. The momentum distributions of SDI and NSDI both strongly depend on the carrier-envelop phase (CEP). Back analysis shows that the ionization times of both electrons in SDI and the recollision time in NSDI have a strong dependence on CEP, which is responsible for the CEP-dependent momentum distributions of SDI and NSDI. The rich details of SDI and NSDI are intuitively revealed by back analysis of the classical trajectories.

1. Introduction

Double ionization (DI) is one of the most important and fundamental processes among various phenomenas of strong field laser-matter interactions. In the past decades, numerous of experimental [1–5] as well as theoretical researches [6–18] have been performed on this area. It has been confirmed that DI can proceed through two different processes, sequential double ionization (SDI) and nonsequential double ionization (NSDI). For SDI, two electrons are ionized one by one independently and no recollision. It can be understood by the tunneling theory based on the single-active-electron approximation [19]. For NSDI, both experimental [2–5,20] and theoretical [21–24] studies have been provided strong evidences that the rescattering mechanism [25] is responsible for it. By this mechanism, the first electron that ionizes through tunneling when the Coulomb barrier is tipped down by the laser electric field is driven back as the electric field reverses its direction and collides with the parent ion inelastically which lead to the second electron being ionized directly or excited with subsequent field ionization [26]. This rescattering mechanism is also responsible for the high-order above threshold ionization [27,28] and high-order harmonic generation [29–33].

In the recent years, strong field DI of atom by an elliptically polarized laser pulse has been performed in experiment and theory. For example, for SDI, in Ref. [1], the experimentally measured semiclassical ionization times in DI of argon and observed intensity-dependent three-band or four-band structures in the ion momentum distributions. Furthermore, these experiment results are well reproduced by the classical model, in Ref. [15]. For NSDI, in Ref. [34], on the basis of a semiclassical model, the authors investigated the momentum distributions of the ion and correlated electron by elliptically polarized laser fields for the various ellipticities and found that all of the successful NSDI events are still as the result of

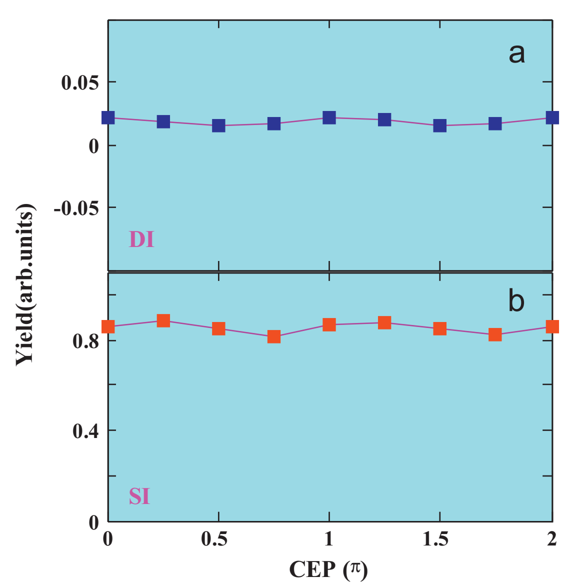

Fig. 1. The total yield of double (a) and single ionization (b) as the function of CEP. The laser intensity is 4.0×10^{14} W/cm^2, the wavelength is 800 nm, the ellipticity ε=0.3 and the pulse duration is 4 cycles.

* Corresponding author. Tel.: +86 13598566928; fax: +86 376 6391760.
E-mail address: hnyubenhai@163.com (B. Yu).

0030-4018/$ - see front matter Crown Copyright © 2013 Published by Elsevier B.V. All rights reserved.
http://dx.doi.org/10.1016/j.optcom.2013.04.029

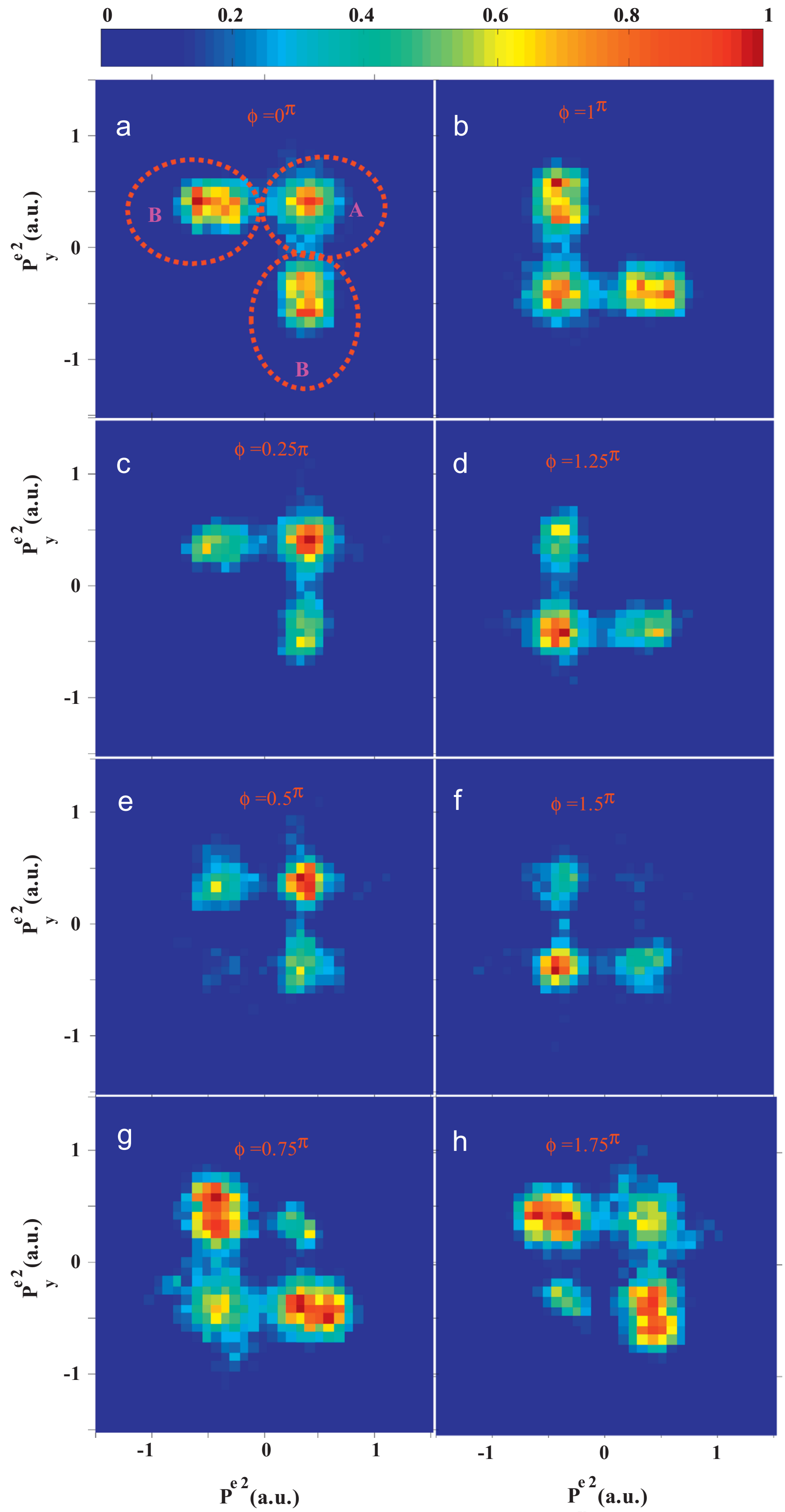

Fig. 2. The momentum distributions of two electrons along the short axis of the laser polarization plane for the trajectories from SDI. The panels (a)–(h) represent CEP $\Phi=0\pi$, 0.25π, 0.5π, 0.75π, 1π, 1.25π, 1.5π and 1.75π, respectively. The laser parameters are same as Fig. 1.

recollision and the main contribution to NSDI no longer comes from the first return of the tunneled electron to its parent ion, as is typical for linear polarization, but from longer orbits for the sufficiently large ellipticity. But so far the dependence of strong field DI for carrier-envelop phase (CEP) in ellipticity few-cycle laser pulse has never been reported, so the microscopic dynamics of electron in this case is obscure.

In this paper, with the classical ensemble model, we investigated strong field DI of xenon atoms by elliptically polarized few-cycle laser pulses. The results show that SDI and NSDI exist simultaneously with this laser pulse. The momentum distributions of two electrons from this two kinds of events strongly depend on CEP. Back analysis shows that the ionization times of both electrons in SDI and the recollision time in NSDI have a strong dependence on CEP, which is responsible for the CEP-dependent momentum distributions of SDI and NSDI. In addition, we find, for NSDI, that the recollision occurs at the first or the second return of the first electron, but not for the third or a later return in the case of elliptically polarized few-cycle laser field.

2. The classical ensemble model

The classical ensemble model has been described detailedly in Ref. [14] and has been used in understanding the physical process of SDI [16] and NSDI [35–40] successfully. In this model, the evolution of two electrons system is governed by Newton's equations of motion [14] (atomic units are used throughout unless stated otherwise):

$$d^2\vec{r}_i/dt^2 = -\vec{\nabla}[V_{ne}(\vec{r}_i) + V_{ee}(\vec{r}_1, \vec{r}_2)] - \vec{E}(t) \quad (1)$$

Where the index $i=1, 2$ refers to the two electrons. $\vec{r}$ represents the two-dimensional (2D) space coordinate, and $\vec{E}(t)$ is the electric field of the elliptically polarized few-cycle laser pulse:

$$\vec{E}(t) = (E_0/\sqrt{\varepsilon^2+1})f(t)[\vec{e}_x \sin(\omega t + \Phi) + \vec{e}_y \varepsilon \cos(\omega t + \Phi)]. \quad (2)$$

where E_0, ε, ω and Φ represent the maximum of the laser electric field, ellipticity, laer frequency and CEP, respectively. Our classical ensemble contains 2×10^6 xenon atoms. In order to obtain enough sub-ensemble for SDI and NSDI, we set $\varepsilon=0.3$. Φ ranging from 0 to 1.75π. $\vec{e}_x$ and $\vec{e}_y$ represent unit vectors along the long and the short axes of the laser polarization plane, respectively. The potentials are

$$V_{ne}(\vec{r}_i) = -2/\sqrt{\vec{r}_i^{\,2} + a^2} \text{ and } V_{ee}(\vec{r}_1, \vec{r}_2) = 1/\sqrt{(\vec{r}_1 - \vec{r}_2)^2 + b^2}, \quad (3)$$

representing the ion–electron and electron–electron interactions, respectively. In the classical model, we employ the softening parameter a to prevent one electron dropping deeply into the Coulomb well and transferring enough energy to the other electron for it to escape the atom [39]. For the ground-state energy of xenon, i.e., −1.23 a.u., the softening parameter must be satisfy $a>1.626$. There is also an upper limit on a. In order to be able to place the two electrons into a classically allowed region with total energy of −1.23 a.u., the softening parameter must satisfy $a<2.112$ [39]. In this paper, we set $a=1.85$. The softening parameter b in the electron–electron interaction is include to avoid the mathematical singularity in our calculations, we set $b=0.05$.

To obtain the initial value, two 2D electrons populated starting from a classically allowed position for the xenon atoms ground-state energy of −1.23 a.u. The initial position of two electrons are situated at (0.95, 0) and (−0.95, 0), respectively. The potential energy at this position is −1.0627 a.u., so the kinetic energy is 0.1673 a.u. The kinetic energy is distributed between the two electrons randomly in the momentum space [21]. Each electron is given the radial velocity only, with sign randomly selected. Then the two electrons are allowed to evolve for a sufficiently long time (100 a.u.) with the absence of the laser field until obtaining the stable position and momentum distribution [40]. Then we turn on the elliptically polarized few-cycle laser pulse. Both Coulomb field and laser field dominate the evolution of the two electrons system. At the end of the laser pulse, we calculate the statistics of DI events which are defined if both electrons achieve the positive energies [21].

We mention that in our classical model, we set the summation of the first and the second ionization potentials of the model atom to be that of the target. In our model atom, the first and the second ionization potentials do not, respectively, match those of the target. However, previous studies have proved that this model is very useful in study double ionization at the qualitative level [16,35,39]. Thus, in this paper we employ this simple model, aiming to have qualitative understanding on the CEP effect of DI in the elliptical laser field.

3. Results and discussions

We calculated DI of xenon atoms by an ellipticity few-cycle laser pulse with the intensity $I=4\times10^{14}$ W/cm^2, wavelength

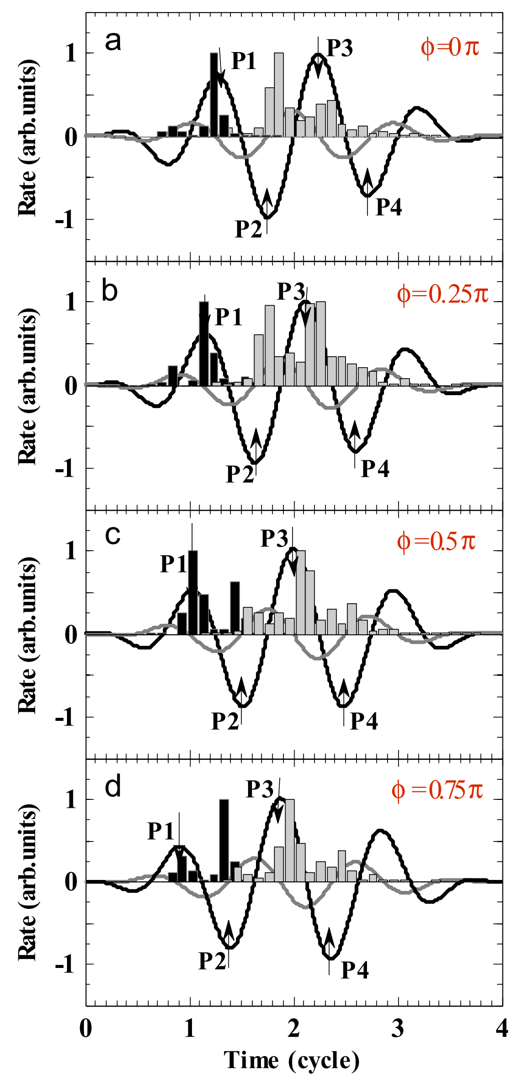

Fig. 3. DI yields versus SI (black) and DI time (gray) for the events from Fig. 2(a)–(d), respectively. The black and gray curves represent the laser fields along the x- and y-axis, respectively.

$\lambda = 800$ nm and the pulse duration is $4T$ (T is the laser cycle). First, in Fig. 1 we show that single and double ionization yields as a function of the CEP. It is clearly seen that both the single and double ionization yields have negligible dependence on the CEP, which is in accord with previous experimental results [41].

Back analysis of the trajectories shows that SDI and NSDI exist simultaneously in DI events, and we separated DI into SDI and NSDI based on the condition whether there are recollisions or not [16]. Fig. 2 displays the momentum distributions of two electrons along the short axis of the laser polarization plane (y-axis) for SDI at eight different CEPs. When CEP $\Phi = 0$, the momenta are mainly distributed in three regions, as shown in Fig. 2(a). Region A locates at the first quadrant, meaning that two electrons emit into the same hemisphere, and regions B locate at the second and fourth quadrants, meaning that two electrons emit into the opposite hemispheres [23]. When $\Phi = 0.25\pi$ and 0.5π, the population primarily in the first quadrant [see Fig. 2(b) and (c)]. While when Φ increases to 0.75π, the momenta mainly distributed in the second and fourth quadrants [see Fig. 2(d)]. Comparing the left and right columns of Fig. 2, one can see a much too similar pattern of trajectories appears every π phase with only an inversion of the axis due to a reversed laser field direction [37].

Consequently, from above analysis, we know that, for SDI, the electron momentum distributions along the y-axis strongly depend on CEP. In order to understand this issue, we trace back the history of the two-electron trajectories. We define the time of single ionization (SI) to be the first time when one of the two electrons obtains positive energy (where the energy includes the kinetic energy and the potential energies of ion–electron and electron–electron interactions), and DI time to be the first time of the two electrons both having positive energies [21].

Fig. 3 displays the SI time (black) and DI time (gray) for $\Phi = 0$, 0.25π, 0.5π and 0.75π, respectively. In Fig. 4 we display the time delay between the final ionization of the first and the second electrons. According to the simple-man model [25], the final momentum is mainly determined by the laser phase at release. When $\Phi = 0$, the first ionization occurs near peak 1 and the dominant part of the second ionization occurs near peak 2 [see Fig. 3(a)]. The time delay between the two ionization steps is $0.5T$, corresponding to the first peak of Fig. 4(a). For these trajectories, the two electrons emit into the opposite hemispheres along the y-axis, responsible for the distribution in regions B of Fig. 2(a). In Fig. 3(a), there also a small part of trajectories, where the second electron ionizes near peak 3. The time delay between the two ionization steps is about $1.0T$ [see the second peak of Fig. 4(a)]. For these trajectories the two electrons emit into the same hemisphere along the y-axis, corresponding to the distribution in region A of Fig. 2(a). When $\Phi = 0.25\pi$, the first ionization still occurs near peak 1, but the number of second ionization near peak 3 becomes great [see Fig. 3(b)]. Suggesting that much more electrons doubly ionized with a time delay $1.0T$ [compare the second peaks of Fig. 4(a) and (b)]. Hence, more electron pairs emit into the same hemisphere compared with the case of $\Phi = 0$, as shown in Fig. 2(b). As CEP increases to 0.5π, the dominate parts of the first and second ionizations occur near peak 1 and peak 3, respectively. The time delay between two ionization steps is about $1.0T$, corresponding to the second peak of Fig. 4(c). For these trajectories the two electrons emit into the same hemisphere, as shown in Fig. 2(c). However, as CEP further increases to 0.75π, it is clearly seen from Fig. 3(d) that the dominate parts of the first and the second ionizations occur near peak 2 and peak 3, respectively. The time delay between two ionization steps is $0.5T$, corresponding to the first peak of Fig. 4(d). For these trajectories, the two electrons emit into the opposite hemispheres [see Fig. 2(d)].

It is more interesting for NSDI. Fig. 5 displays the momentum distributions along the long axis of the laser polarization plane (x-axis). It is clearly seen that the momenta are mainly distributed in the first or third quadrants depending on CEP. This two quadrants both indicate that two electrons emit into the same hemisphere (along $+x$ or $-x$) [40]. Fig. 6 displays the momentum distributions of two electrons along the y-axis. One can see at the various CEPs that the momentum spectra are mainly distributed in

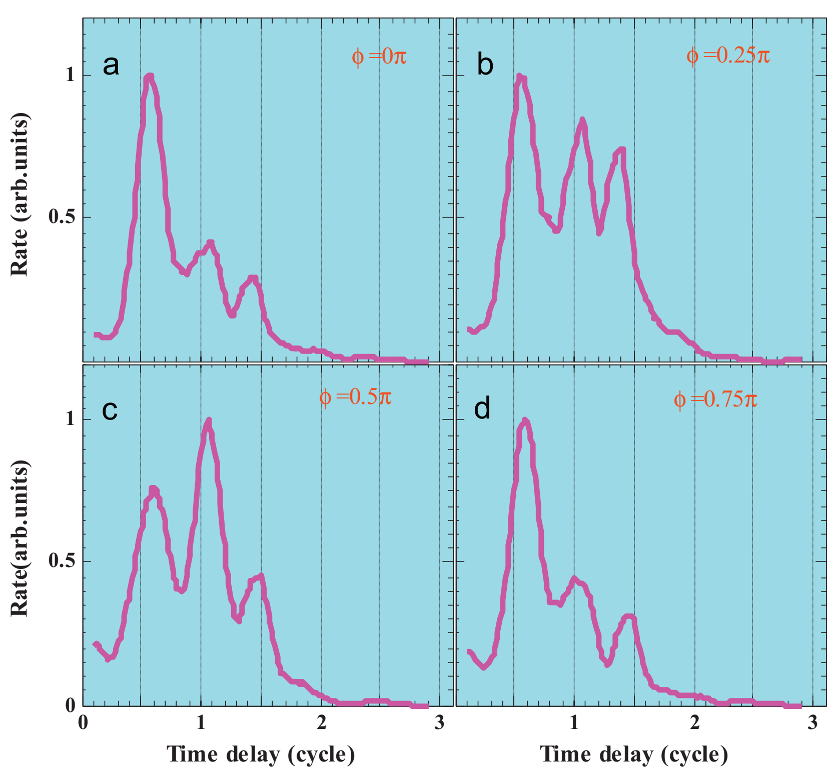

Fig. 4. DI yields versus the time delay between the final ionization of the first and the second electrons for the events from Fig. 3(a)–(d), respectively.

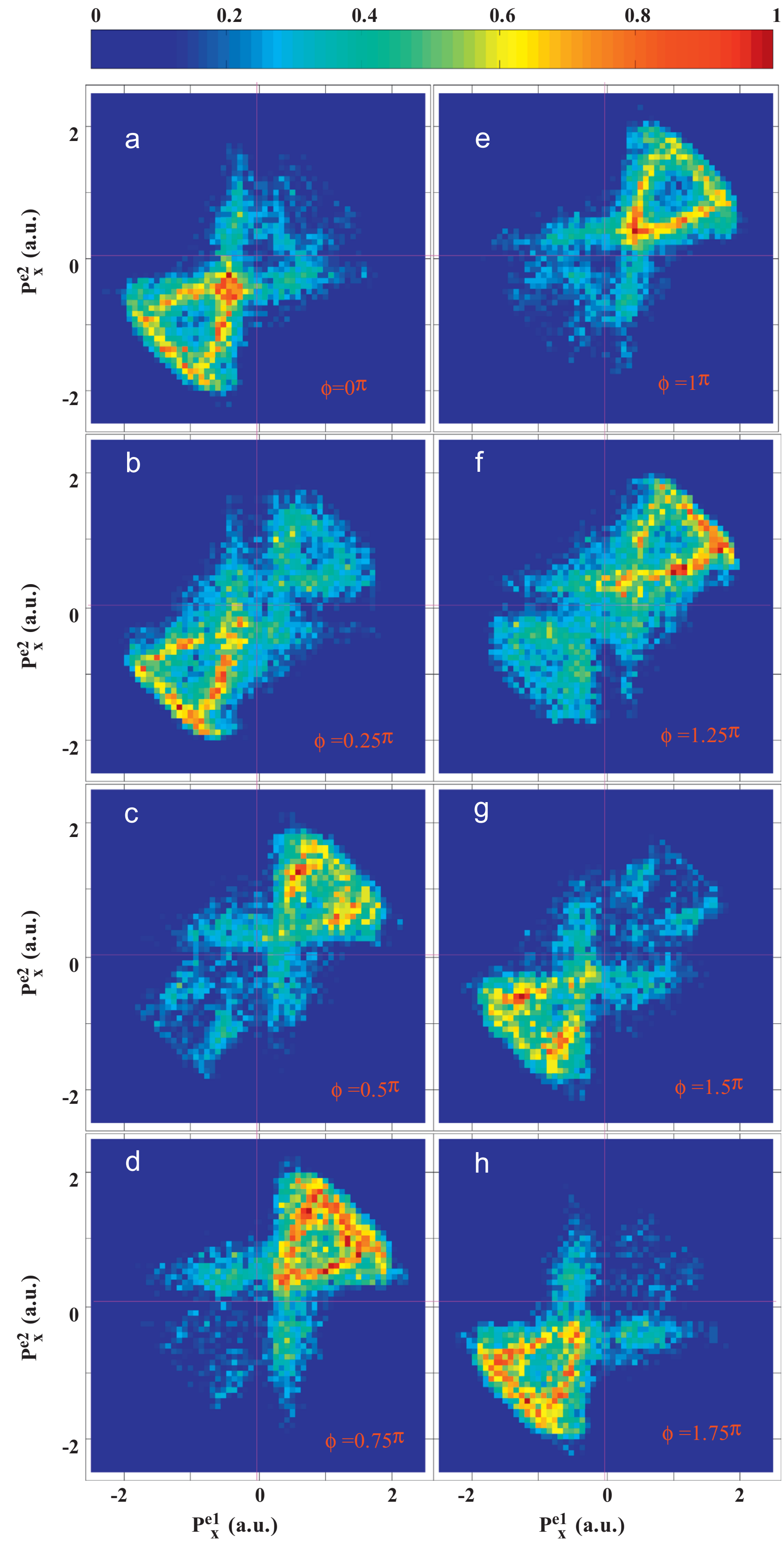

Fig. 5. The momentum distributions of two electrons along the *x*-axis for the trajectories from NSDI and the laser parameters are same as Fig. 2.

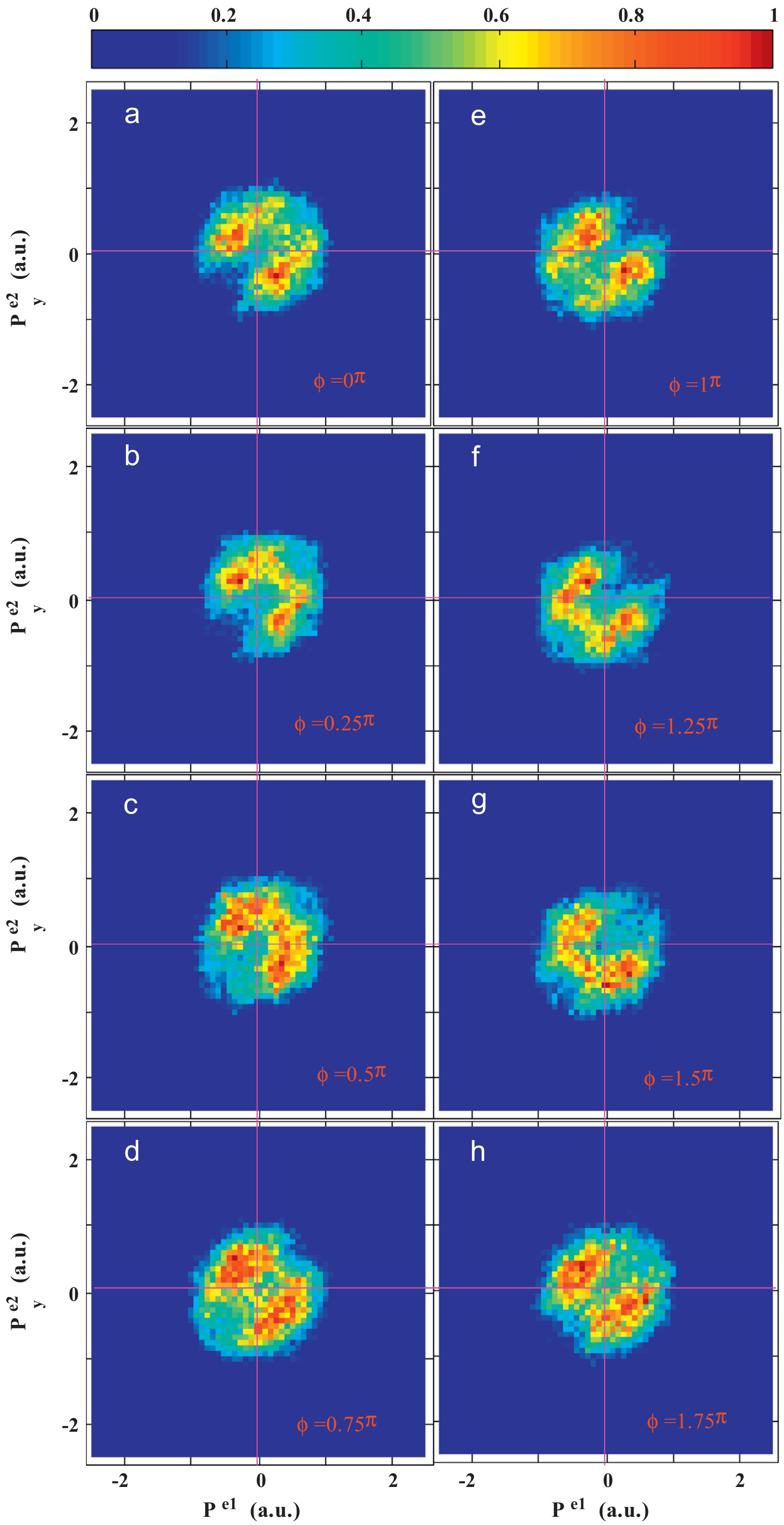

Fig. 6. The momentum distributions of two electrons along the *y*-axis. The panels (a)–(h) correspond to Fig. 5(a)–(h), respectively.

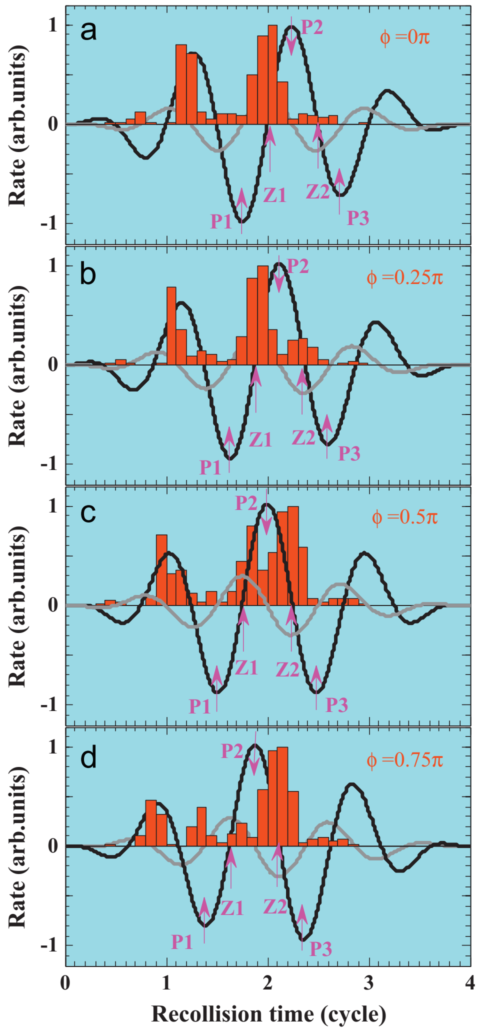

Fig. 7. DI yield versus laser phase at recollision for the events from Fig. 5(a)–(d), respectively. The gray and black curves represent the laser fields in the directions of the *x*- and *y*-axis.

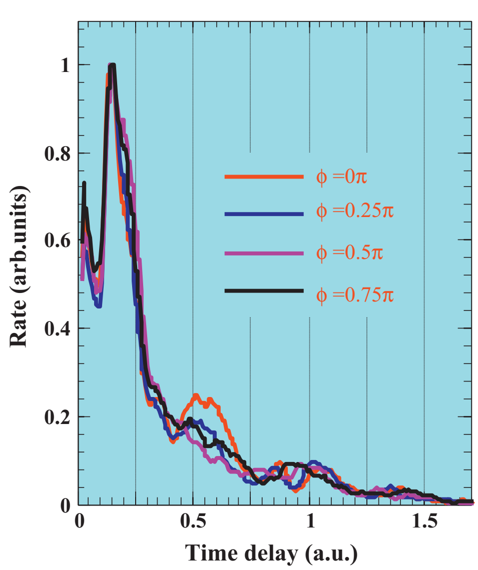

Fig. 8. DI yield versus the time delay between the final ionization of the first and the second electrons after recollision for the trajectories from Fig. 5(a)–(d).

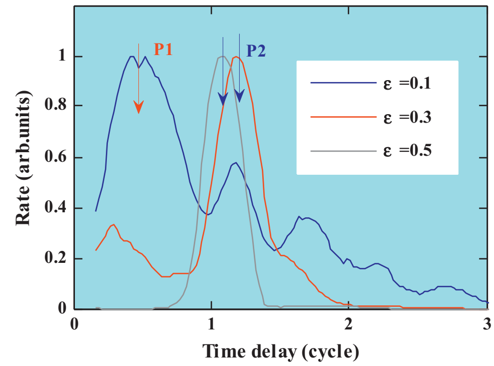

Fig. 9. The rate versus time delay between the single ionization and recollision. The first (i.e., P1) and second (i.e., P2) peaks correspond to the first and second returns of the tunneled electron, respectively.

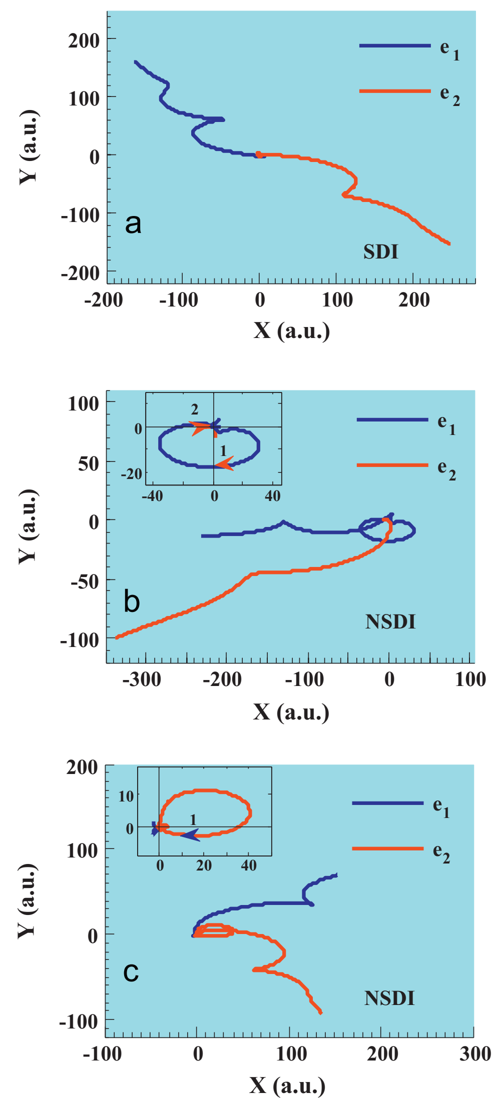

Fig. 10. Three sample space trajectories (a) selected from Fig. 2(a), but (b) and (c) from Fig. 5(a). The insert of panels in (b) and (c) represent the trajectories of tunneled electron from initial to recollision. Furthermore, the arrow and number show the movement direction and the returning times of the electron, respectively.

the second and fourth quadrants which indicates that the two electrons emit into the opposite hemispheres [40]. Both Figs. 5 and 6 exhibit that the much too similar pattern of trajectories appears every π phase which also is due to a reversed laser field direction.

In order to understand the microscopic dynamics of NSDI in elliptically polarized few-cycle laer fields, in Fig. 7 we present the counts of NSDI versus laer phases at recollision for $\Phi=0$, 0.25π, 0.5π and 0.75π, respectively. Here the recollision time is defined to be the instant of the closest approach after the first departure of one electron from the parent core [35]. We refer to the first and the second ionized electrons after recollision as the first and the second electrons below, respectively. In Fig. 8 we display the time delay between the final ionization of the first and the second electrons after recollision, and Fig. 8(a)–(d) correspond to Fig. 7(a)–(d), respectively.

By tracing the NSDI trajectories we find that the most likely scenario for this laser field is that the first electron often ionizes directly at recollision and the second electron often ionizes within $0.25T$ after the first electron ionization (see the first peak in Fig. 8). When $\Phi=0$ and 0.25π, the dominate part of the recollision clusters around the crossing Z1 [see Fig. 7(a)]. For the recollision occurs just before Z1, meaning that the first electron ionizes just before Z1 and the second electron ionizes between Z1 and P2. For these trajectories, the two electrons emit into the same direction (along $-x$) [see Fig. 5(a) and (b)] but emit into the opposite directions along the y-axis [see Fig. 6(a) and (b)]. For the recollision occurs just after Z1, meaning that two electrons ionized between Z1 and P2. For these trajectories the two electrons still emit in the negative direction of the x-axis. In the direction of the y-axis, two electrons still escaped opposite hemispheres as a result of the strong repulsion interaction between the two electrons at recollision. However, as CEP increases to 0.5π and 0.75π, the dominate part of the recollision occurs around the crossing Z2. suggesting that two electrons ionized between P2 and P3. The time delay between two ionization steps is within 0.25 T, corresponding to the first peak in Fig. 8. For these trajectories the two electrons emit into the positive direction along the x-axis [see Fig. 5(c) and (d)]. However, in the direction of the y-axis, for the trajectories that the first electron ionizes between P2 and Z2 and the second electron ionizes between Z2 and P3 which lends that two electrons emit into the opposite hemisphere along the y-axis. But for the trajectories two electrons both ionizes between Z2 and P3, as the strongly repulsion between two electrons which leads two electrons emit into the opposite hemisphere [see Fig. 6(c) and (d)].

We mention that in the linear laser field, recollision often occurs at the first return of the tunneled electron. In our calculations, recollision mainly occurs at the second return, as shown in Fig. 9. For larger ellipticity the contribution from the first return is more strongly suppressed (Fig. 9). This result is consistent with the previous study [34].

Fig. 10 displays the space trajectories of two electrons from the initial to the end of the laser field for SDI and NSDI, and the events from Fig. 2(a) and Fig. 5(a). The insert panels of Fig. 10(b) and (c) show the electron space trajectories from the initial to the recollision for NSDI. In the sub-ensemble, the microscopic dynamics process of SDI is relatively simple, as shown in Fig. 10 (a). But for NSDI, the processes are relatively complicated as the result of the recollision, and the recollision only possible via elliptical trajectories [42]. Trace analysis shows that the electron returns to the parent ion to recollide either at the first returning [see the upper-left panel of Fig. 10(b)] or at the second returning [see the upper-left panel of Fig. 10(c)], but not at the third or later returning in the case of ellipticity few-cycle laser pulse.

At last, we display two sample trajectories in Fig. 11 for the events from Figs. 2(a) and 5(a). In the left column, one electron

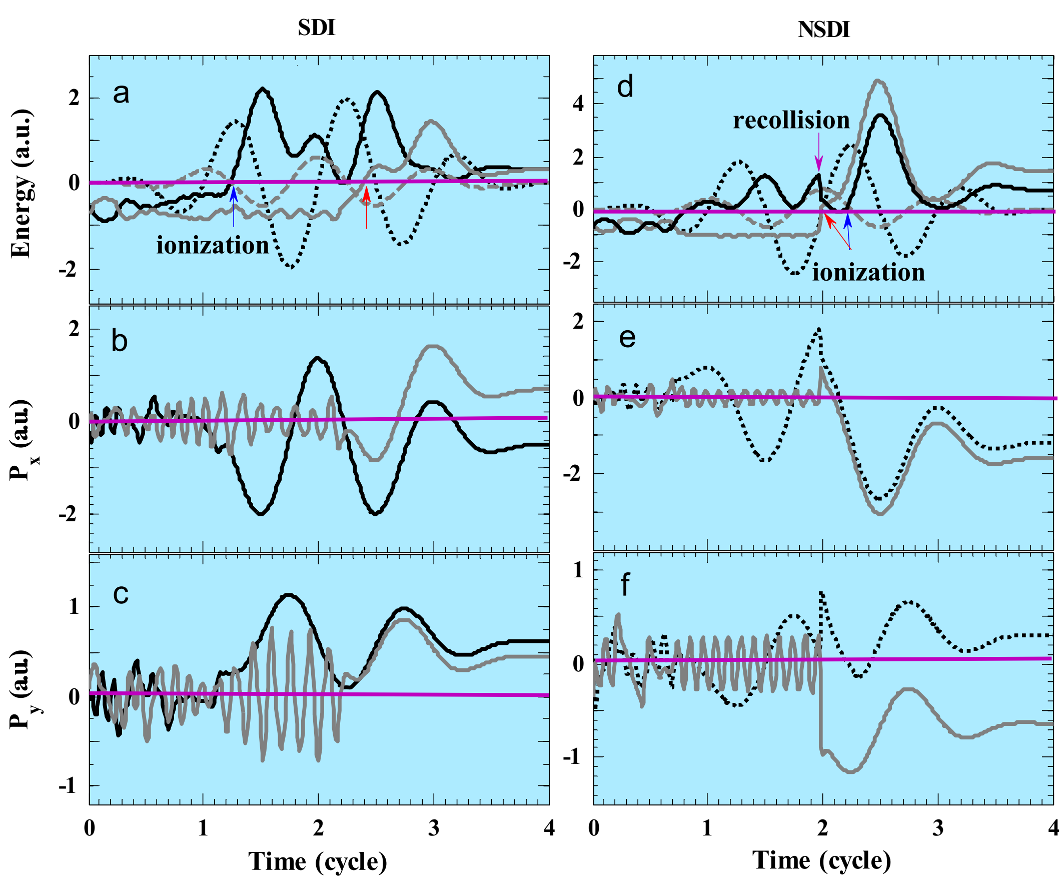

Fig. 11. Two sample trajectories selected from Fig. 2(a) (left column) and Fig. 5(a) (right column), respectively. The upper, middle, and bottom rows show the energy, momentum along the x- and the y-axes versus the time for each electron, respectively. The black dotted and gray dotted curves represent the laser fields along the x- and y-axes, respectively.

ionizes at $1.23T$ [see the black curve in Fig. 11(a)] and the other ionizes at $2.40T$ [see the gray curve in Fig. 11(a)]. The two electrons emit into the opposite hemispheres along the x-axis [see Fig. 11 (b)], but emit into the same hemisphere along the y-axis [see Fig. 11(c)]. In the right column, one electron first ionizes at $0.82T$ then returns to the parent ion to recollide at $1.97T$ transferring the part of energy to the other electron. This process leads that the two electrons ionized simultaneously [see Fig. 11(d)] and emit into the same hemisphere along the x-axis [see Fig. 11(e)]. In the direction of the y-axis, two electrons experience a sudden increase at recollision as a result of the strong electron–electron repulsion force, leading that two electrons emit into the opposite hemispheres [see Fig. 11(f)].

4. Conclusion

In summary, using the classical ensemble model, we have investigated the CEP-dependent strong DI of xenon atoms in elliptically polarized few-cycle laser pulses. In this laser field, both SDI and NSDI exist simultaneously in the DI events, and the momentum distributions for SDI and NSDI have a strong dependence on CEP. By back analyzing the classical trajectories of two electrons, that the ionization times of both electrons in SDI and the recollision time in NSDI strongly depend on CEP, which is responsible for the CEP-dependent momentum distributions of SDI and NSDI. In addition, we find recollision ionization mechanism, i.e., (e, 2e) dominates the NSDI process, and we also found that the recollision occurs at the first return or the second return of the electron but not for the third or a later return because of the short pulse duration.

Acknowledgments

This work was supported by the National Natural Science Foundation of China under Grant Nos. 11005088 and 11047145, the Basic and Advanced Technology of Henan Province of China under Grant Nos. 102300410241 and 112300410021, and the Scientific Research Foundation of Education Department of Henan Province of China under Grant Nos. 2011B140018 and 13A140774.

References

[1] A.N. Pfeiffer, C. Cirelli, M. Smolarski, R. Dörner, U. Keller, Nature 7 (2011) 428.
[2] Th. Weber, H. Giessen, M. Weckenbrock, G. Urbasch, A. Staudte, L. Spielberger, O. Jagutzki, V. Mergel, M. Vollmer, R. Dörner, Nature 405 (2000) 658.
[3] A. Rudenko, V.L.B. De Jesus, Th. Ergler, K. Zrost, B. Feuerstein, C.D. Schröter, R. MoshammerJ Ullrich, Physical Review Letters 99 (2007) 263003.
[4] R. Lafon, J.L. Chaloupka, B. Sheehy, P.M. Paul, P. Agostini, K.C. Kulander, L.F. DiMauro, Physical Review Letters 86 (2001) 2762.
[5] D.N. Fittinghoff, P.R. Boltan, B. Chang, K.C. Kulander, Physical Review Letters 69 (1992) 2642.
[6] M. Lein, E.K.U. Gross, V. Engel, Physical Review Letters 85 (2000) 4707.
[7] Y.M. Zhou, Q. Liao, P.X. Lu, Physical Review Letters 80 (2009) 023412.
[8] Q. Liao, P.X. Lu, Physical Review Letters 82 (2010) 021403(R).
[9] A. Becker, F.H.M. Faisal, Physical Review Letters 84 (2000) 3546.
[10] Y.M. Zhou, Q. Liao, Q.B. Zhang, W.Y. Hong, P.X. Lu, Optics Express 18 (2010) 362.
[11] C.F. Faria, X. Liu, A. Sanpera, M. Lewenstein, Physical Review Letters 70 (2004) 043406.
[12] J.S. Prauzner-Bechcicki, K. Sacha, B. Echhardt, J. Zakrzewski, Physical Review Letters 98 (2007) 203002.
[13] Q. Liao, Y.M. Zhou, C. Huang, P.X. Lu, New Journal of Physic 14 (2012) 013001.
[14] S.L. Haan, L. Breen, A. Karim, J.H. Eberly, Physical Review Letters 97 (2006) 103008.
[15] Y.M. Zhou, C. Huang, Q. Liao, P.X. Lu, Physical Review Letters 109 (2012) 053004.
[16] X. Wang, J.H. Eberly, Physical Review Letters 103 (2009) 103007.
[17] Y.M. Zhou, C. Huang, P.X. Lu, Optics Express 20 (2012) 20201.
[18] A.H. Tong, Y.M. Zhou, Q. Liao, P.X. Lu, Optics Express 18 (2010) 9064.
[19] M.V. Ammosov, N.B. Delone, V.P. Krainov, Soviet Physics—JETP 64 (1986) 1191.
[20] X. Liu, C. Figueira de Morisson Faria, Physical Review Letters 92 (2004) 133006.
[21] Y.M. Zhou, Q. Liao, P.X. Lu, Optics Express 18 (2010) 16025.
[22] S.L. Haan, Z.S. Smith, K.N. Shomsky, P.W. Plantinga, Journal of Physics B 41 (2008) 21102.
[23] Y.M. Zhou, C. Huang, Q. Liao, W.Y. Hong, P.X. Lu, Optics Letters 36 (2011) 2758.
[24] H. Li, J. Chen, H. Jiang, J. Liu, P. Fu, Q. Gong, Z. Yan, B. Wang, Journal of Physics B 42 (2009) 125601.
[25] P.B. Corkum, Physical Review Letters 71 (1993) 1994.
[26] B. Feuerstein, R. Moshammer, D. Fischer, A. Dorn, C.D. Schröter, J. Deipenwisch, J.R. Crespo Lopez-Urrutia, C. Höhr, P. Neumayer, J. Ullrich, H. Rottke, C. Trump, M. Wittmann, G. Korn, W. Sandner, Physical Review Letters 87 (2001) 043003.
[27] M. Lewenstein, K.C. Kulander, K.J. Schafer, P.H. Bucksbaum, Physical Review A 51 (1995) 1495.
[28] D.B. Milošević, G.G. Paulus, D. Bauer, W. Becker, Journal of Physics B 39 (2006) R203.
[29] W. Cao, P. Lu, P. Lan, X. Wang, G. Yang, Physical Review A 74 (2006) 063821.
[30] P. Lan, P. Lu, W. Cao, Y. Li, X. Wang, Physical Review A 76 (2007) 011402(R).
[31] W. Cao, P. Lu, P. Lan, X. Wang, Y. Li, Physical Review A 75 (2007) 063423.
[32] P. Lan, P. Lu, F. Li, Y. Li, Z. Yang, Optics Express 16 (2008) 5868.
[33] W. Cao, P. Lu, P. Lan, Y. Li, X. Wang, Journal of Physics B 41 (2008) 085601.
[34] N.I. Shvetsov-Shilovski, S.P. Goreslavski, S.V. Popruzhenko, W. Becker, Physical Review A 77 (2008) 063405.
[35] Y.M. Zhou, Q. Liao, P.X. Lu, Physical Review A 82 (2010) 053402.
[36] S.L. Haan, J.S. Van Dyke, Z.S. Smith, Physical Review Letters 101 (2008) 113001.
[37] R. Panfili, S.L. Haan, J.H. Eberly, Physical Review Letters 89 (2002) 113001.
[38] C. Huang, Y.M. Zhou, A.H. Tong, Q. Liao, W.Y. Hong, P.X. Lu, Optics Express 19 (2011) 5627.
[39] S.L. Haan, Z.S. Smith, K.N. Shomsky, P.W. Plantinga, Journal of Physics B 42 (2009) 134009.
[40] Y.M. Zhou, C. Huang, A.H. Tong, Q. Liao, P.X. Lu, Optics Express 19 (2011) 2301.
[41] K. O'Keeffe, M. Lezius, European Physical Journal D 37 (2006) 305.
[42] X. Wang, J.H. Eberly, New Journal of Physics 12 (2010) 093407.